

Unidirectional light emission from high- Q modes in optical microcavities

Jan Wiersig

Institut für Theoretische Physik, Universität Bremen, Postfach 330 440, D-28334 Bremen, Germany

Martina Hentschel

*Institut für Theoretische Physik, Universität Regensburg, D-93040 Regensburg, Germany and
ATR Wave Engineering Laboratories, 2-2-2 Hikaridai, Seika-cho, Soraku-gun, Kyoto 619-0228, Japan
(Dated: March 23, 2022)*

We introduce a new scheme to design optical microcavities supporting high- Q modes with unidirectional light emission. This is achieved by coupling a low- Q mode with unidirectional emission to a high- Q mode. The coupling is due to enhanced dynamical tunneling near an avoided resonance crossing. Numerical results for a microdisk with a suitably positioned air hole demonstrate the feasibility and the potential of this concept.

PACS numbers: 42.55.Sa, 42.25.-p, 42.60.Da, 05.45.Mt

Confinement and manipulation of light in microcavities is important for a wide range of research areas and applications, e.g., cavity quantum electrodynamics or novel light sources [1]. A key quantity characterizing a cavity mode is its quality factor $Q = \omega/\Delta\omega$, where ω is the mode frequency and $\Delta\omega$ is the linewidth. A large Q -factor is a basic requirement for low threshold lasing, high sensor sensitivity, narrow wavelength-selective filtering, and strong light-matter interaction. Whispering-gallery modes (WGMs) in microdisks [2], microspheres [3], and microtori [4] have *ultra-high* Q -factors. For state-of-the-art semiconductor microdisks, the record Q -factor is $> 3.5 \times 10^5$ [5, 6]. The applicability of those cavities as microlasers and single-photon sources is, however, limited by isotropic light emission. The best directionality so far is provided by VCSEL-micropillars; see, e.g., Ref. [7]. The emission is *unidirectional* at the cost of a reduced Q -factor, typically well below 10^4 . With present technology, there is a trade-off between Q -factor and directionality.

This dilemma remains when breaking the rotational symmetry of a microdisk. Shape deformation [8, 9] allows improved directionality of emission due to *refractive escape*, but the Q -factors are significantly spoiled. Unidirectional emission has been reported for rounded triangles [10] with $Q \approx 35$ and for spiral-shaped disks [11]. In the latter case, a strong degradation of the cavity Q allows lasing operation only for spirals of the size of conventional edge emitting lasers.

Another approach is to break the symmetry by modifying the evanescent leakage (the optical analogue of tunneling) from WGMs, thereby keeping the high Q -factor. Ref. [12] reported unidirectional lasing from a vertical double-disk structure. Unfortunately, the study was restricted to the near-field pattern. Another suggestion has been to introduce a linear defect into the evanescent inner region of WGMs [13]. Nearly spherical, high- Q fused-silica cavities showed emission into four directions explained by *dynamical tunneling* from a WGM to the exterior of the cavity [14]. Dynamical tunneling is a generalization of conventional tunneling which allows to pass not only through an energy barrier but also through other kinds of dynamical barriers in phase space [15].

In this Letter, we overcome the trade-off between Q -factor and directionality by combining dynamical tunneling and refractive escape. We couple a uniform high- Q mode (HQM)

and a directional low- Q mode (LQM) using enhanced dynamical tunneling near *avoided resonance crossings* (ARCs). ARCs are generalizations of avoided frequency (or energy level) crossings. The latter occurs when the spectrum of a closed system is changed under variation of an external parameter. ARCs appear in open systems, where a complex frequency $\omega - i\Delta\omega/2$ is assigned to each mode. Two types of ARCs can be distinguished [16]. The strong coupling situation exhibits a frequency repulsion and a linewidth crossing upon which the eigenstates interchange their identity. Correspondingly, all spatial mode characteristics such as, e.g., the far-field patterns switch their identity. The weak coupling situation consists of a frequency crossing and a linewidth repulsion. Here, the eigenstates, and also the spatial mode characteristics, do not interchange but only intermix near the crossing point. Moreover, the Q -factors are maintained. Our idea is to exploit this mechanism to "hybridize" a HQM and a directional LQM to a mode with high Q -factor and the directed far-field pattern of the LQM. This idea can be realized in three steps. First, take a cavity with HQMs, e.g., a microdisk. Second, introduce a one-parameter family of perturbations such that at least one HQM is almost unaffected and at least one HQM turns into a LQM having directed emission via refractive escape. Third, vary the parameter such that an ARC occurs between the HQM and the LQM. This scheme allows the systematic design of modes with high Q -factors and highly directed emission.

We demonstrate the applicability of this scheme by a theoretical study of a semiconductor microdisk with a circular air hole as illustrated in Fig. 1. Different versions of such an annular cavity have been studied in the context of quantum chaos [17], optomechanics [18] and dynamical tunneling [19]. The closed system with perfectly reflecting walls has been used as model for dynamical tunneling [20, 21].

Holes with radii $\geq 100\text{nm}$ can be pierced through the disk surface by techniques currently applied to photonic crystal membranes [22]. In Ref. [23] square-shaped holes had been introduced into a GaAs disk to reduce the laser threshold by perturbing the nonlasing modes. Our calculations apply to a small GaAs microdisk of radius $R = 1\mu\text{m}$. Similar disks have been used recently to demonstrate strong coupling between excitons and photons in single quantum dots [24]. We

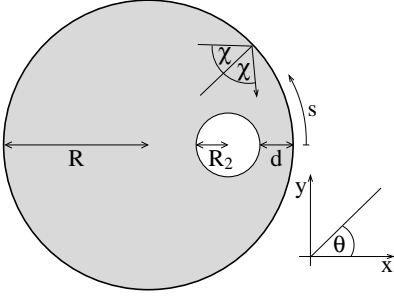


FIG. 1: Schematic top view of the annular cavity with radius R . The radius of the hole is R_2 , the distance to the disk's circumference is d . The direction of the outgoing light is characterized by the angle θ .

choose a slab thickness of 375nm, a temperature of 4K and a free-space wavelength λ close to 900nm. This results in an effective index of refraction $n_{\text{eff}} = 3.3$ for the transverse magnetic polarization with electric field perpendicular to the disk plane. We focus on this polarization, the conclusions are the same for transverse electric polarization.

We use the boundary element method [25] and the S -matrix approach [17] to compute the spatial profile of the electromagnetic field, the Q -factors and the normalized frequencies $\Omega = \omega R/c$, c being the speed of light in vacuum. According to the discrete symmetry, the modes are divided into even and odd symmetry classes.

A WGM in a disk without hole is characterized by azimuthal and radial mode numbers (m, n) . The introduction of a hole modifies a $\text{WGM}_{m,n}$ the stronger the larger n is. This can be seen from the mode in Fig. 2(a) which bears a faint resemblance to a $\text{WGM}_{12,3}$ but is a LQM with directed emission due to refractive escape. In contrast, a $\text{WGM}_{m,n}$ with $n = 1$ is nearly unaffected, see Fig. 2(b). Such modes have high Q -factors and are expected to emit without any preferred direction [13]. Here, we encounter the trade-off between Q -factors and directionality in a single cavity.

We turn now to the realization of an ARC as we vary the parameter d , the minimal distance of the hole to the disk's boundary. Figure 3(a) shows the normalized frequencies of all even-symmetry modes with $\Omega \in [6.97, 7.05]$ corresponding to $\lambda \approx 900\text{nm}$. This figure reveals the typical scenario. For $d/R > 0.35$, WGMs such as $\text{WGM}_{19,1}$ (solid line) and $\text{WGM}_{15,2}$ (dotted) are much less affected by moving the hole than LQMs (dashed). With decreasing d/R all frequencies blueshift since dielectric material is effectively removed from the WGM region. This results in ARCs between WGMs and LQMs, see Figs. 3(a) and (b). At $d/R \approx 0.24$ a frequency repulsion together with a linewidth (Q -factor) crossing takes place. At $d/R \approx 0.42$ we observe a frequency crossing and a linewidth repulsion (cf. inset).

Figure 3(c) shows the directionality U versus d . We define U as the fraction of light emitted into an angular range of $\pm 40^\circ$ around $\theta = 0^\circ$. Remarkably, near the frequency crossing at $d/R \approx 0.423$ the directionality of the $\text{WGM}_{19,1}$ and of the LQM behave in exactly the same way. Gradually decreasing d/R , the directionality of the WGM remains close to that of the LQM until it reaches the maximum at $d/R \approx 0.389$,

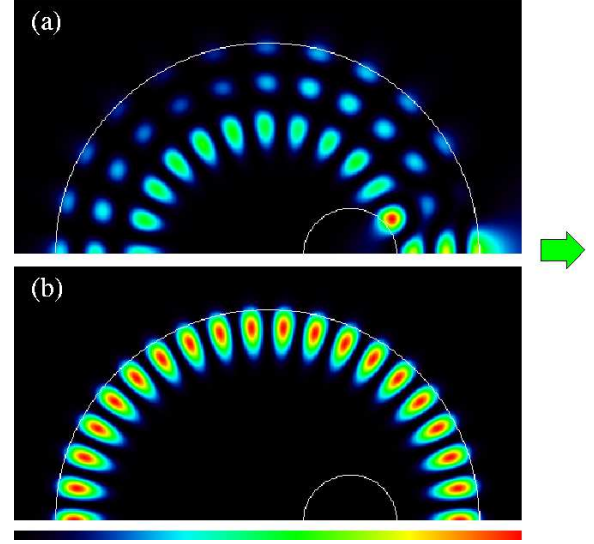


FIG. 2: (Color online) (a) Calculated near-field intensity pattern for LQM, $\Omega = 7.0599$, $Q \approx 300$, even symmetry, $R_2/R = 0.22$ and $d/R = 0.389$. The arrow shows the direction of light emission. (b) $\text{WGM}_{19,1}$, $\Omega = 7.0278$, $Q \approx 553000$.

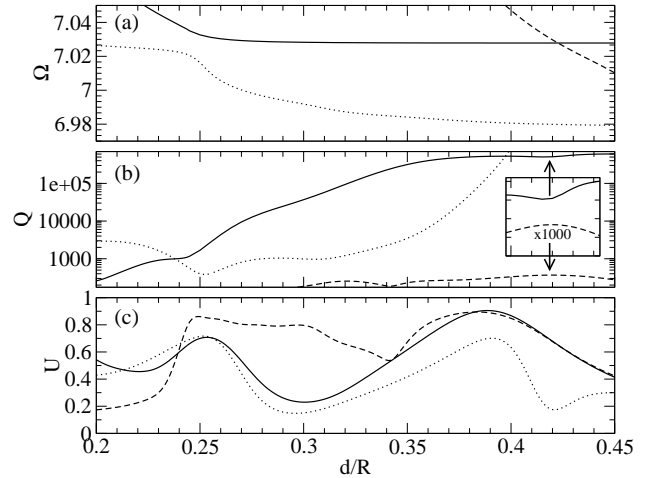


FIG. 3: Normalized frequencies (a) and Q -factors (b) of even-symmetry modes vs. d at fixed $R_2/R = 0.22$. Inset, Q s in linear scale near the linewidth repulsion in the interval $[0.4, 0.44]$. The low- Q branch (dashed) is multiplied by 1000. (c) Fraction U of emitted light into $|\theta| \leq 40^\circ$ for the same modes as in (a) and (b).

where 90% of the light is emitted into a range of $\pm 40^\circ$. Figure 4 shows that at this value of d the angular emission pattern of the WGM and the LQM are almost identical. The far-field pattern has a narrow beam divergence angle of about 57° (full width at half maximum). The spectacular finding is that a WGM with ultra-high $Q \approx 553000$ possesses highly directed emission. The explanation is the hybridization of modes near the ARC. Note that even a small contribution of the LQM to the WGM dominates the far-field pattern because of the strong leakiness of the LQM.

Two additional features in Fig. 3(c) fit naturally into this

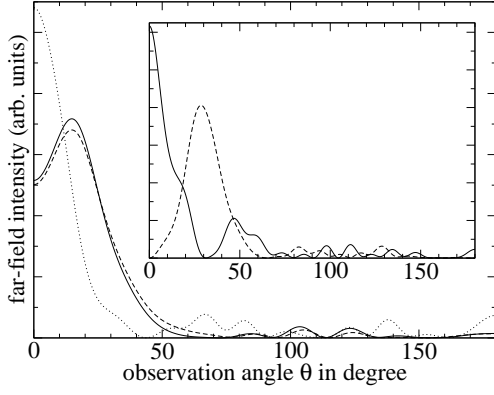


FIG. 4: Angular dependence of the far-field intensity for WGM_{19,1} (solid line) and LQM (dashed) from Fig. 2. Dotted line marks WGM_{34,1}, $d/R = 0.399$, $\Omega = 11.8833$. Inset, even (solid) and odd (dashed) symmetry WGM_{36,1}, $d/R = 0.4478$, $\Omega = 12.5241$.

scheme. First, the directionality of WGM_{15,2}, a spectator of the ARC at $d/R \approx 0.42$, is less affected by the LQM. Second, near the ARC of the WGMs at $d/R \approx 0.24$ the directionalities of both (strongly modified) WGMs are similar.

To see the relation to dynamical tunneling we have to compare mode patterns with ray dynamics. A common approach in the field of quantum chaos is to superimpose the Husimi function (smoothed Wigner function) of a mode onto the Poincaré section [26] as shown in Fig. 5. The Poincaré section restricts the phase space of rays to the outer boundary of the cavity. The remaining variables are $(s, \sin \chi)$ where s is the arclength along the circumference of the disk and χ is the angle of incidence measured from the surface normal; cf. Fig. 1. A good visualisation of the dynamics is achieved by reflecting the rays a finite number of times in the closed cavity with perfectly reflecting outer boundary [17]. The phase space of the annular cavity contains two regular regions defined by $|\sin \chi| > 1 - d/R$. A ray with such a large angle of incidence never encounters the hole. It rotates as whispering-gallery trajectory ($\sin \chi = \text{const}$) clockwise, $\sin \chi > 0$, or counterclockwise, $\sin \chi < 0$. In particular, it cannot enter the region $|\sin \chi| < 1 - d/R$. For small R_2/R , this region is dominated by chaotic trajectories hitting the hole several times and thereby filling this phase space area in a pseudo-random fashion. Embedded into the chaotic region is the leaky region $|\sin \chi| < 1/n_{\text{eff}}$. In the open cavity, a ray entering this region escapes refractively according to Snell's and Fresnel's laws.

The Husimi function of the LQM is restricted to the chaotic part of phase space, see Fig. 5(a). The significant overlap with the leaky region explains the low Q -factor. In contrast, the WGM lives mainly in the regular region, see Fig. 5(b), far away from the leaky region ensuring a high Q . However, a small contribution exists in the chaotic region. To highlight this contribution, the intensity inside the region $|\sin \chi| \leq 1/2$ is multiplied by 5000. The striking similarity to the LQM in Fig. 5(a) carries over to their far-field patterns in Fig. 4.

The role of tunneling is studied through the time evolution of a pure WGM which we define as a wave packet having no contribution in the chaotic region. Such a mode is a su-

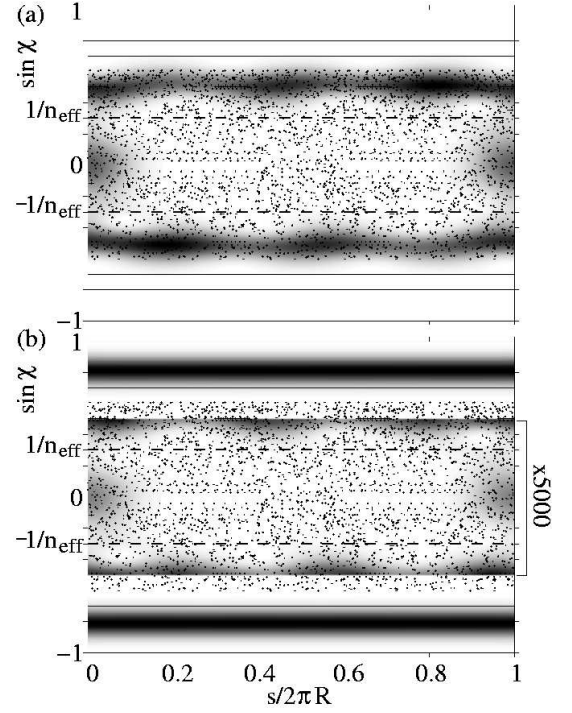


FIG. 5: Poincaré section (dots, solid lines) and Husimi function (shaded regions) of modes in Fig. 2. (a) LQM. (b) WGM_{19,1}, the intensity inside $|\sin \chi| \leq 1/2$ is multiplied by 5000 to allow for a comparison with the LQM. The dashed lines mark the leaky region.

perposition of the real (hybridized) WGM and the LQM in Fig. 5 such that the LQM cancels the chaotic contribution of the real WGM. As time evolves, the initial cancellation vanishes since the LQM component in the superposition is short lived. In other words, a fraction of the initial pure WGM has tunnelled from the regular to the chaotic region which allows for directed emission.

Figure 6(a) shows the directionality for various normalized frequencies Ω . It illustrates that for lower (higher) frequency less (more) peaks appear. This is fully consistent with the fact that the larger the frequency the higher is the density of modes and therefore the larger the number of ARCs.

The best emission directionality we found for WGM_{34,1} with $\Omega \approx 11.88$, which corresponds to $R = 1.7 \mu\text{m}$ at $\lambda \approx 900\text{nm}$ or $R = 1 \mu\text{m}$ at $\lambda \approx 530\text{nm}$. The maximum in U is at $d/R = 0.399$, see Fig. 6(a). The far-field pattern is shown in Fig. 4 as dotted line. The emission is unidirectional with an angular divergence of 28° which is much smaller than the values reported for rounded triangles (90°) [10] and spiral-shaped disks (60°) [11], and only 50% larger than that of a VCSEL-micropillar of the same radius [7]. The Q -factor is so huge that our numerics is pushed to the limit; as a conservative lower bound we estimate $Q \approx 10^8$. In practise, this theoretical bound for the Q -factor is unreachable nowadays due to absorption [2] and surfaces roughness [27], i.e. the introduction of the hole does not affect the experimental Q -factor.

Figure 6(b) reveals that the directionality depends only weakly on the hole radius. This behaviour allows rather large

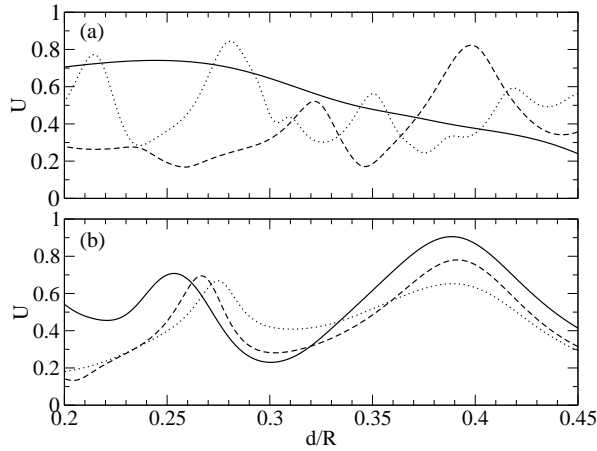


FIG. 6: (a) Directionality vs. d for various frequencies Ω at fixed $R_2/R = 0.22$. $\text{WGM}_{15,1}$ with $\Omega \approx 5.71$ (solid line), $\text{WGM}_{34,1}$ with $\Omega \approx 11.88$ (dashed), $\text{WGM}_{38,1}$ with $\Omega \approx 13.16$ (dotted). (b) $\text{WGM}_{19,1}$ for various hole radii: $R_2/R = 0.22$ (solid), 0.28 (dashed), and 0.315 (dotted).

fabrication tolerances without compromising the directionality much.

Let us now briefly turn to the odd symmetry modes. Since the ARC scenario is different for even and odd symmetry, the respective far-field patterns will differ. For low n WGMs, the introduction of a hole only slightly lifts the even-odd degen-

eracy present in a perfect disk. Hence, a light emitter couples easily to both WGMs which possibly leads to less directed emission. This problem is resolved in the following cases: (i) In realistic microdisks, the degeneracy is lifted due to Rayleigh scattering from the boundary [6]. (ii) For a single-photon source it is desirable to place a single emitter (e.g. a quantum dot) on an antinode of an optical mode in order to enhance light-matter interaction. In such a case, the emitter does not couple to the other-symmetry mode which has zero intensity there. (iii) It is possible to find pairs of ultra-high- Q WGMs showing simultaneously highly directed output, see inset in Fig. 4. In this particular case, the far-field maxima are displaced from each other which is interesting for applications like all-optical switches and sensors.

Finally, the angular divergence of the output beam in vertical direction can be estimated to be $2/\sqrt{m}$ as in the case of an ideal disk [28]. For our examples with $m = 19, 34, 38$ follow angular divergences of $26.3^\circ, 19.7^\circ, 18.6^\circ$.

In summary, we presented a new and general concept to achieve unidirectional light emission from high- Q modes in microcavities utilizing resonance-enhanced dynamical tunneling. For a pierced microdisk, we showed unidirectional emission from modes with ultra-high $Q > 10^8$.

We would like to thank T. Harayama, S. Shinohara, S. Sunada, H. Lohmeyer, N. Baer, and F. Jahnke for discussions. J.W. acknowledges financial support by the Deutsche Forschungsgemeinschaft.

-
- [1] K. J. Vahala, *Nature* **424**, 839 (2003).
 - [2] S. L. McCall, A. F. J. Levi, R. E. Slusher, S. J. Pearton, and R. A. Logan, *Appl. Phys. Lett.* **60**, 289 (1992).
 - [3] L. Collot, V. Lefevre-Seguin, M. Brune, J. Raimond, and S. Haroche, *Europhys. Lett.* **23**, 87 (1993).
 - [4] V. S. Ilchenko, M. L. Gorodetsky, X. S. Yao, and L. Maleki, *Opt. Lett.* **26**, 256 (2001).
 - [5] K. Srinivasan, M. Borselli, T. J. Johnson, P. Barclay, P. Painter, A. Stintz, and S. Krishna, *Appl. Phys. Lett.* **86**, 151106 (2005).
 - [6] M. Borselli, K. Srinivasan, P. E. Barclay, and P. Painter, *Appl. Phys. Lett.* **85**, 3693 (2004).
 - [7] H. Rigneault, J. Broudic, B. Gayral, and J. M. Gérard, *Opt. Lett.* **26**, 1595 (2001).
 - [8] A. F. J. Levi, R. E. Slusher, S. L. McCall, S. J. Pearton, and R. A. Logan, *Appl. Phys. Lett.* **62**, 561 (1993).
 - [9] J. U. Nöckel and A. D. Stone, *Nature* **385**, 45 (1997).
 - [10] M. S. Kurdoglyan, S.-Y. Lee, S. Rim, and C.-M. Kim, *Opt. Lett.* **29**, 2758 (2004).
 - [11] M. Kneissl, M. Teepe, N. Miyashita, N. M. Johnson, G. D. Chern, and R. K. Chang, *Appl. Phys. Lett.* **84**, 2485 (2004).
 - [12] D. Y. Chu, M. K. Chin, W. G. Bi, C. W. Tu, and S. Ho, *Appl. Phys. Lett.* **65**, 3167 (1994).
 - [13] V. M. Apalkov and M. E. Raikh, *Phys. Rev. B* **70**, 195317 (2004).
 - [14] S. Lacey, H. Wang, D. H. Foster, and J. U. Nöckel, *Phys. Rev. Lett.* **91**, 033902 (2003).
 - [15] M. J. Davis and E. J. Heller, *J. Chem. Phys.* **75**, 246 (1981).
 - [16] W. D. Heiss, *Phys. Rev. E* **61**, 929 (2000).
 - [17] M. Hentschel and K. Richter, *Phys. Rev. E* **66**, 056207 (2002).
 - [18] H. Schomerus, J. Wiersig, and M. Hentschel, *Phys. Rev. A* **70**, 012703 (2004).
 - [19] G. Hackenbroich and J. U. Nöckel, *Europhys. Lett.* **39**, 371 (1997).
 - [20] S. D. Frischat and E. Doron, *Phys. Rev. E* **57**, 1421 (1998).
 - [21] O. Bohigas, D. Boosé, R. Eydio de Carvalho, and V. Marville, *Nucl. Phys. A* **560**, 197 (1993).
 - [22] A. Badolato, K. Hennessy, M. Ataïre, J. Dreiser, E. Hu, P. M. Petroff, and A. Imamoglu, *Science* **308**, 1158 (2005).
 - [23] S. A. Backes, J. R. A. Cleaver, A. P. Heberle, J. J. Baumberg, and K. Köler, *Appl. Phys. Lett.* **74**, 176 (1999).
 - [24] E. Peter, P. Senellart, D. Martrou, A. Lemaitre, J. Hours, J. M. Gérard, and J. Bloch, *Phys. Rev. Lett.* **95**, 067401 (2005).
 - [25] J. Wiersig, *J. Opt. A: Pure Appl. Opt.* **5**, 53 (2003).
 - [26] M. Hentschel, H. Schomerus, and R. Schubert, *Europhys. Lett.* **62**, 636 (2003).
 - [27] A. I. Rahachou and I. V. Zozoulenko, *J. Appl. Phys.* **94**, 7929 (2003).
 - [28] B. J. Li and P.-L. Liu, *IEEE J. Quantum Elect.* **33**, 1489 (1997).